International Journal of Engineering Trends and Technology
ISSN: 2231-5381/ https://doi.org/10.14445/22315381/IJETT-V73I3P120

Volume 73 Issue 3, 265-273, March 2025

Original Article

Optimization of Fatigue Response in Notched AISI 316L Friction Welded Joints Using a Hybrid Entropy-VIKOR-Taguchi Approach

Jagadesh Kumar Jatavallabhula[1], Vaddi Venkata Satyanarayana[2], Vasudeva Rao Veeredhi[3]

[1, 3]*Department of Mechanical, Bioresources and Biomedical Engineering, College of Science, Engineering and Technology, University of South Africa, Florida Campus, Johannesburg, South Africa.*
[2]*Department of Mechanical Engineering, Vidya Jyothi Institute of Technology, Aziznagar, Hyderabad, India.*

[1]*Corresponding Author : jagadeshkumar82@gmail.com*

Received: 24 September 2024 Revised: 13 January 2025 Accepted: 20 February 2025 Published: 28 March 2025

Abstract *- Current research investigates the effect of notch geometric parameters, viz. width, depth, and central angle, on the fatigue life and stress amplitude of friction-welded AISI 316L stainless steel joints. Despite the extensive use of friction welding, a critical gap exists in understanding how notch geometry influences fatigue performance in engineering applications. The current study addresses this gap by employing a hybrid Entropy-VIKOR-Taguchi technique to optimize fatigue life and minimize stress amplitude. Fatigue specimens were prepared from friction-welded rods according to ASTM E606 standards, with varying notch geometries based on a Taguchi L9 orthogonal array. The un-notched specimen exhibited a fatigue life of 5285 cycles, while notched specimens showed a range from 150 to 1627 cycles. The maximum stress amplitude required to maintain a strain amplitude of 0.3% is 486.70 MPa for the un-notched specimen, whereas, for the notched specimens, it ranges between 332.76 and 540.99 MPa. Optimal parameters were identified as mid-level notch width and depth with a low central angle, leading to a significant improvement in fatigue life and reduced stress amplitude. The ANOVA results show that the notch central angle contributes the most to the overall optimization of the responses, accounting for 31.55%, followed by notch depth at 29.10% and notch width at 20.85%.*

Keywords *- Fatigue, Notch, VIKOR, Stress amplitude, Strain amplitude, Scanning electron microscope.*

1. Introduction

Friction welding is a highly efficient solid-state joining method renowned for its exceptional ability to fuse dissimilar metals with superior quality [1, 2]. Robert et al. explored the benefits of using Linear Friction Welding (LFW) for fabricating high-value components in the aero industry and underscored the reliability of joints produced through LFW. It was reported that friction-welded joints displayed good fatigue response, unlike fusion-welded joints [3]. Wang et al. investigated the fatigue behaviour of LFW weathering steels with high phosphorus content using digital image correlation. It was reported that ductile fracture occurred at the base metal part, with LFW joint efficiency being almost 100% and fatigue strength of joints being comparable to that of the base metal [4]. Opricovic and Tzeng invented the MCDM technique known as VIKOR, which is used to select and rank alternatives based on conflicting criteria. VIKOR aims to find a compromise solution that provides the best overall performance, considering both the "maximum group utility" and "minimum individual regret" principles. The technique has been widely applied in various fields to effectively support decision-making processes by handling complex and conflicting criteria [5]. The VIKOR technique, an MCDM tool, helps rank and choose the best option from alternatives with conflicting criteria. Its objective is to find a compromise solution closest to the Positive-Ideal Solution (PIS) and farthest from the negative-ideal solution. The process involves identifying key evaluation criteria, assessing alternatives, and using an Lp-metric as an aggregating function to determine the optimal ranking based on relative closeness to the PIS [6]. In the study by Dev et al., the Entropy-VIKOR method was used for material selection in automotive piston components. The Entropy approach calculated criteria weights like density, hardness, and wear rate, while VIKOR ranked composites based on mechanical and tribological properties. Through steps such as determining alternatives, constructing a decision matrix, and identifying criteria weights, the optimal material (A-3 with 6% porcelain) was identified as the best for the intended application [7]. Ashiwani Kumar et al. investigated the wear properties of Cr-reinforced AA7075 alloy composites, utilizing the Hybrid Entropy-VIKOR method to analyze and rank material compositions. The VIKOR

technique facilitated decision-making by providing a comprehensive ranking of the composites, which is essential for selecting the most suitable materials for specific structural and tribological applications in industries such as automotive and aerospace [8]. In the study conducted by Yadav et al., eleven performance-defining attributes of dental composites were considered, and the weight criteria of these attributes were calculated using the Entropy method.

VIKOR method was used to rank the dental composites, with DHZ6 obtaining Rank 1, followed by DHZ8, DHZ4, DHZ2, and DHZ0. Entropy-VIKOR method is popular in the biomedical field owing to its ability to handle complex decision-making situations [9]. Chandrasekar et al. undertook multi-response optimization of parameters in electrochemical machining to maximize material removal rate and minimize overcut and delamination in micro-drilling AA6061-TiB_2 in situ composites. The entropy-VIKOR method was used to optimize the conflicting responses, and the optimal parameters were determined to be an electrolyte concentration of 2 mol, an applied voltage of 16V, and a current of 4A. It was concluded that the concentration of electrolytes had the highest impact on the VIKOR index, followed by applied voltage and current [10]. Ashiwani Kumar et al. examined the synergistic impact of SiC/marble dust reinforcing particulates on the wear characteristics of hybrid alloy composites, and optimization of sliding wear was carried out using the Taguchi approach. Subsequently, materials were ranked based on performance measures using the hybrid ENTROPY-VIKOR method. The results indicated that the SM-62 alloy composite demonstrated superior overall performance compared to other composites [11].

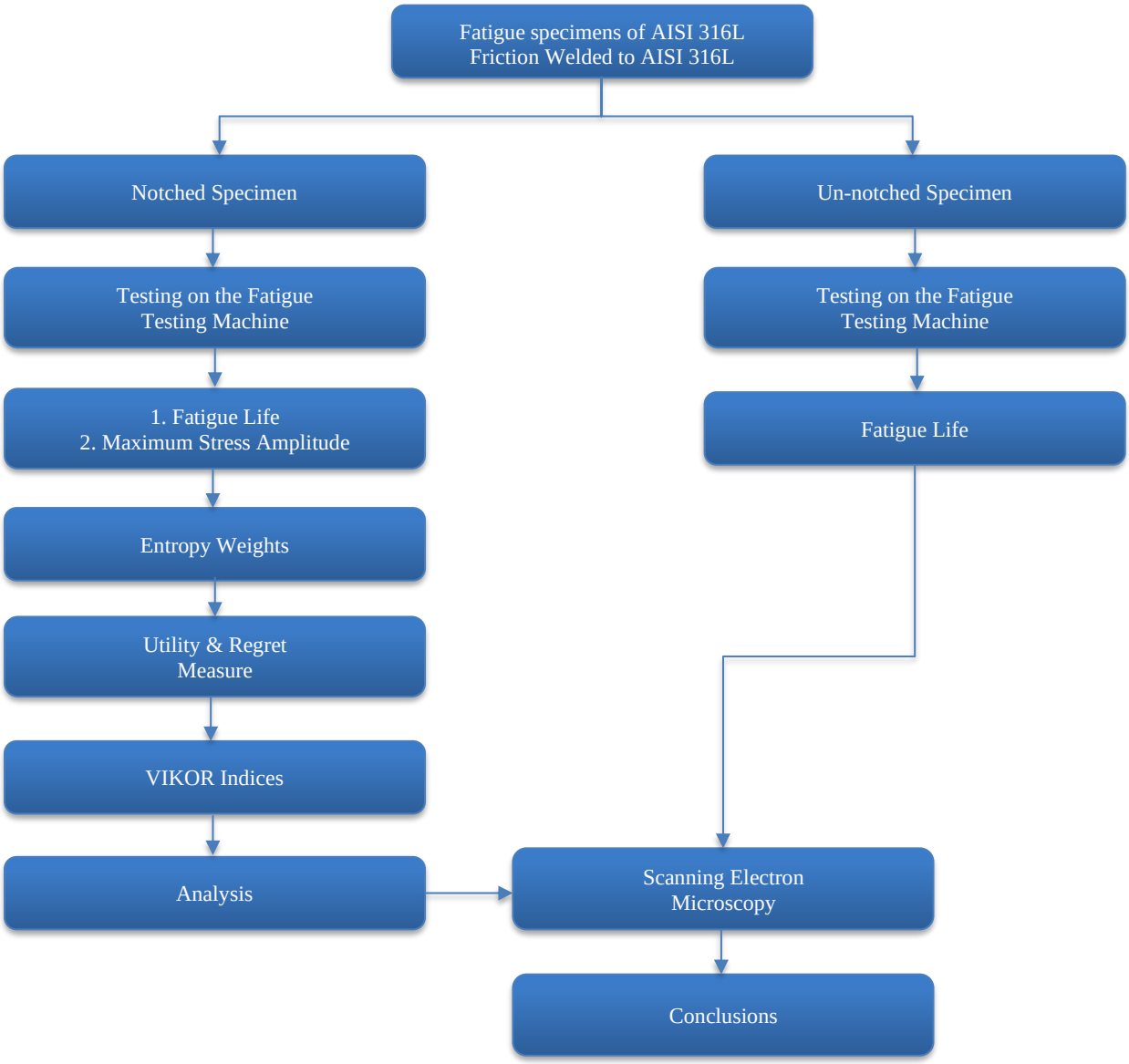

Fig. 1 Flowchart of the research work

Rajesh Kumar et al. merged Entropy weight and VIKOR measurement methods to optimize process parameters during the EDM of Al-18% SiCp Metal matrix composite. The investigation focused on analyzing the impacts of pulse on time, peak current, and flushing pressure on responses like material removal rate, tool wear rate, radial overcut, and surface roughness with the goal of attaining a singular optimal solution. The single optimal solution for the EDM process was achieved by objectively analyzing and weighting multiple criteria [12]. Ali Jahan et al. developed a modified VIKOR methodology for selecting materials in engineering design, addressing the limitations of existing methods.

The proposed method aimed to improve the material selection results in different applications, particularly in biomedical applications where implant materials are expected to have comparable properties to human tissues. The proposed method was compared to traditional VIKOR and other decision-making methods, demonstrating its effectiveness in producing ranking orders and prioritizing materials in engineering design processes [13]. Tara Sasanka et al. applied the VIKOR method to select the most suitable magnesium alloy for automotive applications, highlighting the critical role of material selection in improving vehicle performance, reducing CO_2 emissions, and enhancing fuel economy. The study evaluated eight magnesium alloys across ten properties, using three weighting methods: equal, unequal, and entropy-based factors. VIKOR was employed to rank the alloys and guide the decision-making process. The results demonstrated the effectiveness of the VIKOR method in identifying the optimal magnesium alloy and suggested its applicability for material selection in other industries [14]. Even though extensive research has been conducted on the fatigue behaviour of friction welded joints, particularly focusing on un-notched specimens, the influence of notch geometry on fatigue performance in AISI 316L stainless steel remains largely underexplored.

Moreover, the application of MCDM tools like the VIKOR method in optimizing fatigue life with notch geometric parameters is yet to be explored. This gap presents a significant opportunity to enhance our understanding of notched fatigue behaviour, which is critical for real-world applications in industries where mechanical joints face complex stress conditions, such as in marine, aerospace, and biomedical applications. The critical influence of notch geometry on fatigue life and stress amplitude for AISI 316L friction welded joints is investigated by using Taguchi L_9 OA for exploring alternatives, which are then weighted by the Entropy method. Subsequently, the VIKOR method is employed to identify the best and worst alternatives among them.

This novel hybrid approach can prove to be a superior technique for optimizing fatigue response in welded joints. Fatigue life and maximum stress amplitude for un-notched and notched specimens were measured using strain-controlled testing on an Instron 8801 machine. The research work is visually represented through a flowchart in Figure 1.

2. Materials and Methods

2.1. Material

AISI 316L austenitic stainless steel is distinguished by its high chromium and low carbon content when compared to other AISI 300 family steels. This possesses exceptional corrosion resistance even under adverse circumstances, and because of this, it is extensively utilized in applications where exposure to corrosive substances occurs frequently. It is also used in various structural and manufacturing applications due to its high ductility, strength, and stability at high temperatures [15, 16]. The current work comprises a notch fatigue analysis of AISI 316L friction welded joints. The chemical composition and mechanical properties of AISI 316L austenitic stainless steel are tabulated in Tables 1 and 2, respectively.

Table 1. Chemical composition (wt %)

Element	C	Si	Mn	P	S	Cr	Mo	Ni	Fe
Composition	0.02	0.468	1.238	0.04	0.01	16.613	2.09	10.19	Balance

Table 2. Mechanical properties of AISI 316L

Modulus of Elasticity (GPa)	**Brinell Hardness (HBW)**	**Tensile Strength (MPa)**	**Poisson's Ratio**
193	184	719	0.27

2.2. Friction Welding

Friction welding is a solid-state welding method that removes welding defects, including undercuts, cracking, porosity, slag inclusions, and lack of fusion, which are present in conventional welding methods. Friction welding does not require fully melting the metal surfaces at the junction [17]. Additionally, the pollutants at the weld junction's surface are removed upon first contact with the specimen, saving money and removing the need for surface cleaning. The other benefits, like superior mechanical properties, have contributed to the successful widespread adoption of Friction Welding [18].

A 150 KN friction welding machine manufactured by ETA Technology is employed in the current work, and it has the provision to vary the welding parameters. The parameters used during the friction welding of AISI 316L rods of 14 mm diameter are tabulated in Table 3. The joints made after welding are shown in Figure 2. The burn-off material formed as a flash at the interface is removed before further processing.

Table 3. Parameters used during friction welding

Name of the Parameter	The Magnitude of the Parameter	Units
Friction Force	5	KN
Forge Force	10	KN
Burn off	5	mm
Spindle Speed	1500	rpm

Fig. 2 AISI 316L friction welded to AISI 316L

2.3. Fatigue Testing

The material under consideration is subjected to cyclic loading in marine applications, and fatigue testing is carried out. ASTM E606 is a test standard for determining the fatigue properties of metallic materials under uniaxial cyclic loading in a strain-controlled method. The test typically involves preparing standardized specimens and subjecting them to cyclic loading until failure occurs.

2.3.1. Fatigue Testing Machine

Fatigue testing is conducted on 100kN Instron 8801 Servo Hydraulic Fatigue Testing Machine. The machine employed is shown in Figure 3, which provides changing strain amplitude and the facility to read the fatigue life and maximum stress amplitude directly applied during the test. The strain amplitude in the current research was maintained at 0.3% for all the specimens.

2.3.2. Fatigue Specimen

The chosen stainless steel has a high composition of chromium that provides superior corrosion resistance; hence, it is used popularly in marine components. The sea waves cause low cycle fatigue on the components, and therefore, it is necessary to study the fatigue response under various crack conditions. The welded joints (Figure 2), which were prepared on a friction welding machine, were taken to make test specimens. The fatigue specimens were prepared as specified by the ASTM E606 standard on CNC lathe and CNC milling machines. The cracks are artificially created in the form of notches on the specimens in the current investigation. The specimen drawing and the V-notch geometric parameters, i.e. Width (w), Depth (d) and Notch Central Angle (a), are presented in Figures 4 and 5, respectively. The un-notched and notched specimens (Run 1 to Run 9) after fabrication on the CNC Lathe and CNC Milling machines are presented in Figure 6.

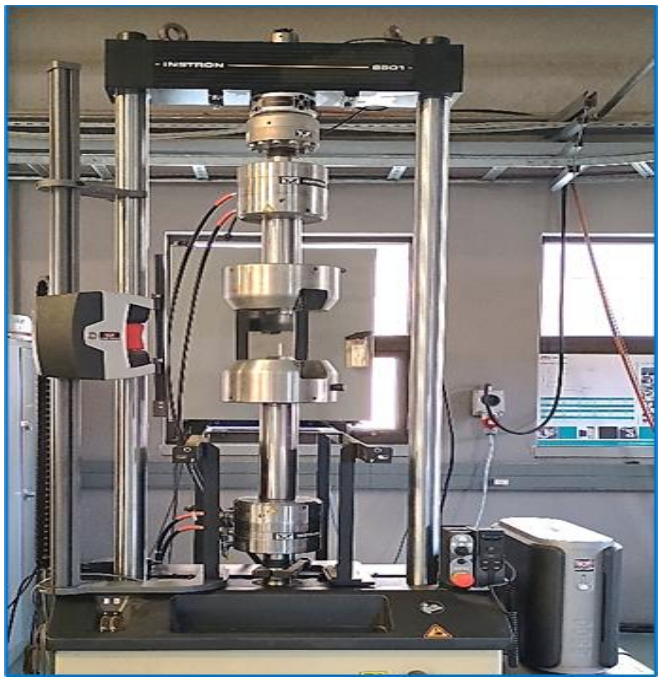

Fig. 3 100kN Instron 8801 servo hydraulic fatigue testing machine

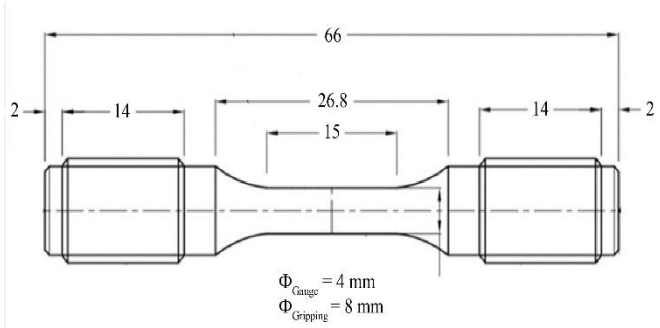

Fig. 4 Specimen drawing

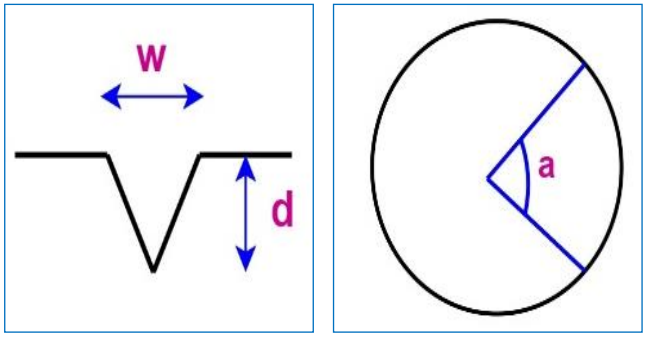

(a) Width and depth **(b) Central angle**

Fig. 5 Notch parameters

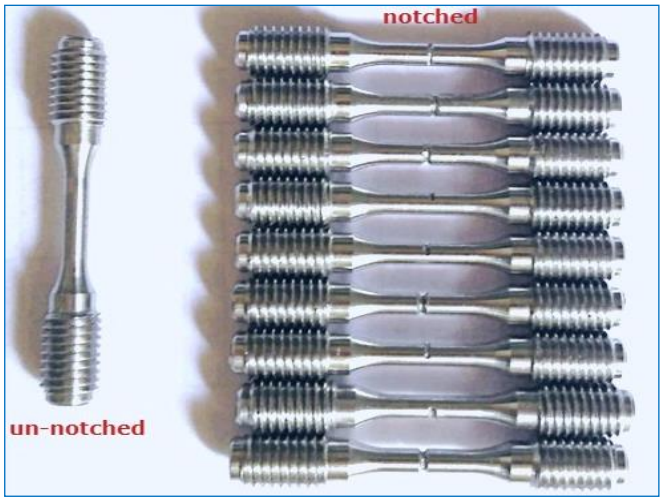

Fig. 6 Un-notched and notched (run 1 to run 9 from top to bottom) specimens

2.4. Scanning Electron Microscopy

The Zeiss Crossbeam 550 SEM, equipped with advanced imaging and focused ion beam technology, is employed for high-resolution imaging and detailed microstructural analysis. Through SEM fractography, researchers can precisely pinpoint the initiation point of fractures and track crack propagation, which is critical for studies involving fatigue and creep behaviour. The fractured specimens, after fatigue testing, were ultrasonically cleaned, degassed and kept in the chamber of the SEM machine for fractography to determine the failure mode.

2.5. Design of Experiments

2.5.1. Taguchi Method

The notch geometry created on specimens viz width, depth and notch central angle are the factors each at three levels, chosen in the current research and tabulated in Table 4. Taguchi L_9 OA with nine different factors combination is presented in Table 5. A full factorial design with the same factors offers good accuracy and resolution but requires 27 experimental runs, making it cumbersome, time-consuming, and costly to implement. Therefore, the L_9 array, which provides a reasonable balance of accuracy and efficiency, was chosen for this study. The robustness and consistency of the experimental results were ensured by conducting multiple repetitions of each experiment and reporting the average of the best two outcomes.

Table 4. Factors chosen and their levels

Factor Chosen	Notation Used	Units	Levels of the Factors		
			Low (-1)	Medium (0)	High (1)
Width	w	mm	1.00	1.25	1.50
Depth	d	mm	0.50	0.75	1.00
Notch Central Angle	a	Degrees	120º	240º	360º

Table 5. Notch parameters used for fatigue investigation

Run	Absolute Values			Coded Values		
	w (mm)	d (mm)	a (degrees)	w	d	a
1	1	0.5	120º	-1	-1	-1
2	1	0.75	240º	-1	0	0
3	1	1	360º	-1	1	1
4	1.25	0.5	240º	0	-1	0
5	1.25	0.75	360º	0	0	1
6	1.25	1	120º	0	1	-1
7	1.5	0.5	360º	1	-1	1
8	1.5	0.75	120º	1	0	-1
9	1.5	1	240º	1	1	0

2.5.2. Responses Measured

The responses in the current investigation are Fatigue life and Maximum Stress Amplitude induced in the specimen during the test. The objective of the investigation is to maximize the fatigue life and minimize the stress amplitude induced in the specimen. The experiments are designed to minimize the VIKOR indices, yielding the overall optimality condition.

2.5.3. Entropy Weight

Entropy is the term used in the information theory of probability in the context of either getting or losing information from a source. The probability so obtained is taken as weight with respect to the total information.

The current investigation takes the responses and the number of experiments to compute the weights. The results x_{ij} represent the magnitudes of the responses, i = 1, 2,.....m and j= 1, 2.....n. The experiments m=9, and the number of responses n=2 are used in the current investigation. The entropy and weights are computed employing Equations (1) to (3).

- First, the normalized 'p' values for the indicators are found using Equation (1).

$$p_{ij} = \frac{x_{ij}}{m + \sum_{i=1}^{m} x_{ij}^2} \quad (1)$$

- Next, the value of the entropy for each indicator is calculated using Equation (2).

$$e_j = -\sum_{i=1}^{m}\left[p_{ij} \times \ln\left(p_{ij}\right)\right] - \left[1 - \sum_{i=1}^{m} p_{ij}\right] \times \ln\left(1 - \sum_{i=1}^{m} p_{ij}\right) \quad (2)$$

- Finally, the weights of each indicator are found using the Equation (3).

$$w_j = \frac{1 - e_j}{\sum_{j=1}^{m}(1 - e_j)} \quad (3)$$

2.5.4. VIKOR Method

VIKOR method is applicable to multi-response conditions implemented using the following steps, and the optimal value is found, which yields the lowest VIKOR index.

- The results are converted into the decision matrix, i.e. $D[x_{ij}]_{m\times n}$, where D is the decision matrix, and x_{ij} is the j^{th} attributes results of the i^{th} alternatives. The decision matrix can be expressed as;

$$D = \begin{bmatrix} x_{11} & x_{12} & \dots & x_{1n} \\ x_{21} & x_{22} & \dots & x_{2n} \\ x_{31} & x_{32} & \dots & x_{3n} \\ \vdots & \vdots & \vdots & \vdots \\ x_{m1} & x_{m2} & \dots & x_{mn} \end{bmatrix} \quad (4)$$

where i = 1,2,3,4,…m & j = 1,2,3,4,….n

- The decision matrix is normalized by Equations (5) and (6), respectively, for maximising and minimising the output responses.

$$n_{ij} = \frac{x_{ij} - \min(x_{ij})}{\max(x_{ij}) - \min(x_{ij})} \quad (5)$$

$$n_{ij} = \frac{\max(x_{ij}) - x_{ij}}{\max(x_{ij}) - \min(x_{ij})} \quad (6)$$

where i = 1,2,3,4,…m & j = 1,2,3,4,….n

- Calculate the utility measure S_i values according to the Equation (7);

$$S_i = \sum_{j=1}^{n} (w_j n_{ij}) \quad (7)$$

Where w_j is weight associated with the j^{th} criterion.

- Calculate the regret measure R_i values using the Equation (8).

$$R_i = \max [w_j n_{ij}] \quad (8)$$

- The VIKOR indices are computed using $\vartheta = 0.5$ employing the Equation (9).

$$Q_i = \vartheta \frac{S_i - \min S_i}{\max S_i - \min S_i} + (1 - \vartheta) \frac{R_i - \min R_i}{\max R_i - \min R_i} \quad (9)$$

ϑ in Equation (9), is the weight of the strategy for "group utility" (compromise solution) versus "individual regret" in the decision-making process.

3. Results and Discussion

The tensile strengths of the un-notched and notched friction welded joints were evaluated and are presented in Table 6. The un-notched joint exhibited a tensile strength of 649 MPa, while the notched joint showed a reduced strength of 568 MPa. The reduction of tensile strength between un-notched and notched specimens can be attributed to the reduction in cross-sectional area. In comparison, the base material had a tensile strength of 719 MPa. The weld bead is wide at the centre and thin at the periphery of the weld joint Figure 7 due to variations of forge pressure along the interface of the joint. Further, a fine grain structure was formed at the centre due to dynamic recrystallization, and a coarse grain structure was formed at the periphery of the joint due to higher temperature [19].

However, the overall bonding between metals was good, and hence, the reduction of tensile strength of base material from 719 MPa to that of weld joint of 649 MPa is not large. The fatigue life and maximum stress amplitude induced for the un-notched and notched specimens are compiled in Tables 7 and 8, respectively, by testing on multiple samples; among them, the average of the best two trials is taken for analysis.

It is found that the un-notched welded specimen yields a fatigue life of 5285 cycles, and the maximum stress amplitude induced is 486.70 MPa at a strain amplitude of 0.3%. The fatigue life of the welded specimens, with notches of various geometries created at the weld joint interface, is in the range of 150-1627 cycles, and the stress amplitude induced is in the range of 332.76-540.99 MPa. In Run 3, when the notch is deep to a larger extent and continued throughout the periphery, the fatigue life was reduced to a discernible level due to generating more stress concentration zones at the root of the notch. The maximum stress amplitude generated in the material was only 335.42 MPa, and in the subsequent cycles, it reduced gradually due to a reduction in strength of the material.

A similar condition was observed in Run 9 when the notch was deep but did not continue throughout the periphery; it yielded a better fatigue life of 810 cycles. Stress-induced variation was due to the variation in the cross-section area of the specimen and the variation in geometries of notches. The stress amplitude induced in the material reduced successively at the end of each cycle upon cyclic loading due to a reduction in the strength of the material. The SEM image (Figure 8) of a typical notched specimen (Run 9) has exhibited failure along the grain boundary due to the presence of austenite during the application of cyclic loading. SEM reveals characteristic striations and beach marks developed during cyclic loading. There is a clear visibility of both dimples and cleaved surfaces in the micrograph; however, more regions are dominated by dimples. Therefore, the failure seems more ductile and less brittle as the material possesses superior ductility.

Table 6. Tensile strengths of friction welded joints (MPa)

Un-Notched Specimen	Notched Specimen
649	568

Table 7. Results of un-notched friction Welded AISI 316L specimen

Run	Max. Stress Amplitude (MPa)	Fatigue Life (cycles)
No Notch	486.70	5285

Table 8. Results of notched friction welded AISI 316L specimens

Run	Max. Stress Amplitude (MPa)	Fatigue Life (cycles)
1	474.66	1385
2	364.97	828
3	335.42	150
4	540.99	1627
5	374.51	436
6	381.10	801
7	332.76	781
8	404.96	804
9	332.76	810

The normalized results of Fatigue Life and Maximum Stress Amplitude are computed as per the VIKOR method with the objective of achieving higher fatigue life and lower stress amplitude induced in the material. The Equations (5) and (6) are employed to convert the test results into normalised results, which are furnished in Table 9. The entropy and the subsequent weights for the results are calculated for Fatigue Life and Maximum Stress Amplitude employing the Equations (1)-(3) and are presented in Table 10. The weightage for fatigue life is 0.503 while for Maximum stress amplitude is 0.497 respectively.

The entropy obtained for fatigue life is 0.008 and this indicates that the experimental results obtained are homogeneous in nature. This homogeneity helps predict the fatigue life at other parameter combinations in the set domain more accurately. The utility measure, regret measure, and VIKOR index are computed per the VIKOR method employing Equations (6)-(8) and are furnished in Table 11. The VIKOR method ranks the alternatives based on the indices starting from the minimum value.

Table 9. Normalized results of the responses

Run	Fatigue Life	Maximum Stress Amplitude
1	0.836	0.319
2	0.459	0.845
3	0.000	0.987
4	1.000	0.000
5	0.194	0.800
6	0.441	0.768
7	0.427	1.000
8	0.443	0.653
9	0.447	1.000

Table 10. Entropy and weights of the responses

Parameter	Entropy	Weights
Fatigue Life	0.008	0.503
Max. Stress Amplitude	0.018	0.497

Thus, the alternative presented in Run 8 (VIKOR index of 0.1219) is found to be the best alternative from the VIKOR method. In MCDM techniques, a compromise solution is obtained by integrating the maximum utility and minimum regret with varying values of ϑ. In the current research, a value of 0.5 is used for ϑ so that equal weight is given to both group utility and individual regret.

The VIKOR indices are subjected to standard ANOVA employing Yate's algorithm [20, 21] and the variation that occurred due to factors and errors due to lack of fit are presented in Table 12. It is evident from the ANOVA that the notch central angle contributes to 31.55%, followed by notch depth at 29.10%, followed by notch width at 20.85%, for minimising the VIKOR indices.

The assumption in the ANOVA is that both responses viz. Fatigue Life and Max. Stress Amplitude follows normal population distribution with equal variance. The "SS" of notch factors in Table 12 represents the variations among the runs, while the "SS" of error represents the variation within the sample of items undertaken for each run. The error component cropped due to chance causes only, and the assignable causes did not play any role in the investigation.

Table 11. Utility index, regret index and VIKOR index

Run	Utility Measure	Regret Measure	VIKOR Index
1	0.5787	0.4202	0.4579
2	0.6513	0.4205	0.6156
3	0.4911	0.4911	0.4677
4	0.5026	0.5026	0.5248
5	0.4952	0.3977	0.2136
6	0.6036	0.3820	0.4039
7	0.7122	0.4974	0.9642
8	0.5474	0.3250	0.1219
9	0.7221	0.4974	0.9856

Table 12. ANOVA of VIKOR indices

Source	DOF	SS	MS	Contribution %
w	2	0.1449	0.07246	20.85
d	2	0.2023	0.10114	29.10
a	2	0.2193	0.10966	31.55
Error	2	0.1285	0.06427	--
Total	8	0.6951	--	--

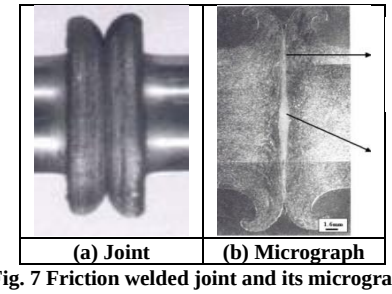

(a) Joint **(b) Micrograph**

Fig. 7 Friction welded joint and its micrograph

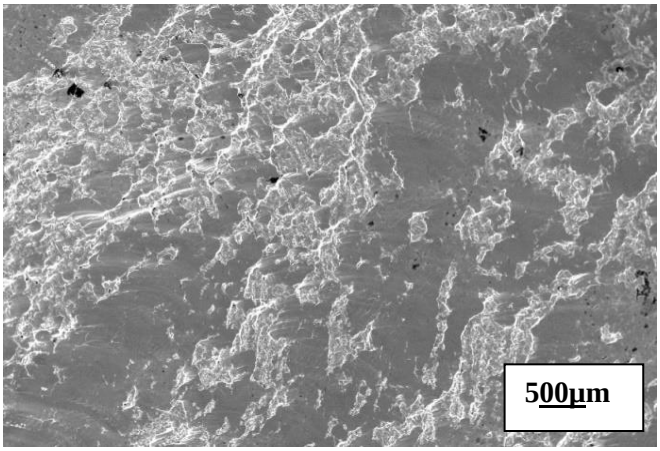

Fig. 8 Scanning electron micrograph of friction welded AISI 316L after fatigue failure

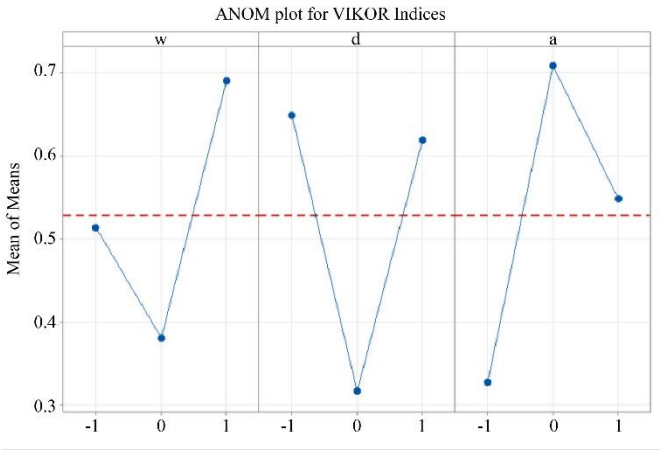

Fig. 9 ANOM plot for VIKOR indices

Fig. 10 Specimen of the confirmation experiment after fatigue failure

Table 13. Results of the confirmation experiment

Notch Parameters			Fatigue Life (cycles)	Maximum Stress (MPa)
w	d	a		
0	0	-1	1530	520.5

The ANOM plot for VIKOR indices is presented in Figure 9. The VIKOR method advocates the minimal index value while arriving at the optimality condition. It is evident from ANOM that the optimal parameter condition is width and depth are at their mid-levels, while the notch central angle is at the low level. The optimal parameter condition from the ANOM is computed as notch width and depth at mid-levels and notch central angle at the lowest level, i.e. w=1.25 mm, d = 0.75 mm and a = 120º. A confirmation experiment is conducted under the optimal parameters condition, and the results are presented in Table 13. The specimen of the confirmation experiment after fatigue failure is presented in Figure 10. The Entropy – VIKOR – Taguchi hybrid technique has yielded satisfactory results that arrive at the optimal condition. It is found that Run 5 of the OA, is of the same width and depth when compared to the optimal condition. The only difference observed is in the central angle; Run 5 has a = 360º while the optimal condition has a = 120º. It is evident that fatigue life increased significantly from 436 cycles of Run 5 to 1530 cycles with the reduction in the notch central angle.

4. Conclusion

The fatigue investigation on notched AISI 316L friction-welded joints using the hybrid Entropy-VIKOR-Taguchi techniques produced promising results. The un-notched specimen showed a fatigue life of 5285 cycles, while the notched specimens ranged from 150 to 1627 cycles. The optimal parameters (mid-level notch width and depth, low central angle) yielded a fatigue life of 1530 cycles, significantly improving over Run 5 (436 cycles), with the difference attributed to the notch central angle. ANOVA revealed that the notch central angle had the most influence (31.55%) on fatigue life, followed by depth (29.10%) and width (20.85%). These findings are crucial for aerospace, marine, and biomedical industries where fatigue performance is critical. Future research should apply this hybrid approach to different materials and configurations, with the potential integration of machine learning for enhanced predictive capabilities. The hybrid Entropy-VIKOR-Taguchi method can be further extended by combining it with other MCDM techniques like TOPSIS or AHP to evaluate comparative performance and refine optimization strategies.

Acknowledgments

The authors thank the University of South Africa for providing an opportunity to undertake the current research as part of the postdoctoral research program. The authors also thank the Head of the Mechanical Engineering Department, Vidya Jyothi Institute of Technology, for the valuable suggestions given during the research work.

Abbreviations

VIKOR : VIekriterijumsko KOmpromisno Rangiranje
MCDM : Multi-Criteria Decision-Making
ANOVA : Analysis of Variance
SS : Sum of squares
MS : Mean squares
DOF : Degrees of freedom
SEM : Scanning Electron Microscope
OA : Orthogonal Array

References

[1] A. Seshu Kumar et al., "Evaluation of Bond Interface Characteristics of Rotary Friction Welded Carbon Steel to Low Alloy Steel Pipe Joints," *Materials Science and Engineering: A*, vol. 824, 2021. [CrossRef] [Google Scholar] [Publisher Link]

[2] Rajendra Goud et al., *Chapter 11-Welding and Joining of Novel Materials*, Automation in Welding Industry: Incorporating Artificial Intelligence, Machine Learning and Other Technologies, pp. 183-213, 2024. [CrossRef] [Google Scholar] [Publisher Link]

[3] Robert Owsinski et al., "Characterisation of Joint Properties through Spatial Mapping of Cracks in Fatigue Specimens, Extracted from the Linearly Friction Welded Steel Coupon," *Precision Engineering*, vol. 71, pp. 78-89, 2021. [CrossRef] [Google Scholar] [Publisher Link]

[4] Yixun Wang et al., "Microstructure, Mechanical Properties and Fatigue Behaviours of Linear Friction Welded Weathering Steels," *International Journal of Fatigue*, vol. 159, 2022. [CrossRef] [Google Scholar] [Publisher Link]

[5] Abbas Mardani et al., "VIKOR Technique: A Systematic Review of the State of the Art Literature on Methodologies and Applications," *Sustainability*, vol. 8, no. 1, pp. 1-38, 2016. [CrossRef] [Google Scholar] [Publisher Link]

[6] Shankar Chakraborty, Prasenjit Chatterjee, and Partha Protim Das, *Multi-Criteria Decision-Making Methods in Manufacturing Environments*, Apple Academic Press, 2023. [Google Scholar] [Publisher Link]

[7] Sanni Dev, Amit Aherwar, and Amar Patnaik, "Material Selection for Automotive Piston Component Using Entropy-VIKOR Method," *Silicon*, vol. 12, no. 1, pp. 155-169, 2020. [CrossRef] [Google Scholar] [Publisher Link]

[8] Ashiwani Kumar, Mukesh Kumar, and Piyush Chandra Verma, "Ranking Analysis of AA7075-Cr Alloy Composites Based on Physical, Mechanical, and Sliding Wear Assessment Using Hybrid Entropy-VIKOR Approach," *International Journal of Metal Casting*, vol. 18, no. 1, pp. 352-372, 2024. [CrossRef] [Google Scholar] [Publisher Link]

[9] Ramkumar Yadav et al., "Selection and Ranking of Dental Restorative Composite Materials Using Hybrid Entropy-VIKOR Method: An Application of MCDM Technique," *Journal of the Mechanical Behaviour of Biomedical Materials*, vol. 147, 2023. [CrossRef] [Google Scholar] [Publisher Link]

[10] S. Chandrasekhar, and N.B.V. Prasad, "Multi-Response Optimization of Electrochemical Machining Parameters in The Micro-Drilling of AA6061-Tib2in Situ Composites Using the Entropy-VIKOR Method," *Proceedings of the Institution of Mechanical Engineers, Part B: Journal of Engineering Manufacture*, vol. 234, no. 10, pp. 1311-1322, 2020. [CrossRef] [Google Scholar] [Publisher Link]

[11] Ashiwani Kumar, Mukesh Kumar, and Bhavna Pandey, "Investigations on Mechanical and Sliding Wear Performance of AA7075-SiC/Marble Dust/Graphite Hybrid Alloy Composites Using Hybrid Entropy-VIKOR Method," *Silicon*, vol. 14, no. 5, pp. 2051-2065, 2022. [CrossRef] [Google Scholar] [Publisher Link]

[12] Rajesh Kumar Bhuyan, and Bharat Chandra Routara, "Optimization the Machining Parameters by Using VIKOR and Entropy Weight Method during EDM Process of A-18% Sicp Metal Matrix Composite," *Decision Science Letters*, vol. 5, no. 2, pp. 269-282, 2016. [CrossRef] [Google Scholar] [Publisher Link]

[13] Ali Jahan et al., "A Comprehensive VIKOR Method for Material Selection," *Materials and Design*, vol. 32, no. 3, pp. 1215-1221, 2011. [CrossRef] [Google Scholar] [Publisher Link]

[14] C. Tara Sasanka, and K. Ravindra, "Implementation of VIKOR Method for Selection of Magnesium Alloy to Suit Automotive Applications," *International Journal of Advanced Science and Technology*, vol. 83, no. 5, pp. 49-58, 2015. [CrossRef] [Google Scholar] [Publisher Link]

[15] Xiang Jian-Yang, Song Ren-Ba, and Hou Dong-Po, "Characteristics of Mechanical Properties and Microstructure for 316L Austenitic Stainless Steel," *Journal of Iron and Steel Research International*, vol. 18, no. 11, pp. 53-59, 2011. [Google Scholar] [Publisher Link]

[16] Jay M. Korde, Akhil V. Sreekumar, and Balasubramanian Kandasubramanian, "Corrosion Inhibition of 316L-Type Stainless Steel Under Marine Environments Using Epoxy/Waste Plastic Soot Coatings," *SN Applied Sciences*, vol. 2, no. 7, pp. 1-13, 2020. [CrossRef] [Google Scholar] [Publisher Link]

[17] Namrata Gangil et al., "Linear Friction Welding of Similar and Dissimilar Materials: A Review," *Metals and Materials International*, vol. 31, pp. 1-21, 2024. [CrossRef] [Google Scholar] [Publisher Link]

[18] Dipen Kumar Rajak et al., "Friction-Based Welding Processes: Friction Welding and Friction Stir Welding," *Journal of Adhesion Science and Technology*, vol. 34, no. 24, pp. 2613-2637, 2020. [CrossRef] [Google Scholar] [Publisher Link]

[19] F.C. Liu, and T.W. Nelson, "Grain Structure Evolution, Grain Boundary Sliding and Material Flow Resistance in Friction Welding of Alloy 718," *Materials Science and Engineering: A*, vol. 710, pp. 280-288, 2018. [CrossRef] [Google Scholar] [Publisher Link]

[20] Douglas C. Montgomery, *Design and Analysis of Experiments*, 4th ed., John Wiley & Sons, pp. 1-720, 1996. [Google Scholar] [Publisher Link]

[21] Angela Dean et al., *Handbook of Design and Analysis of Experiments*, CRC Press, pp. 1-960, 2015. [Google Scholar] [Publisher Link]